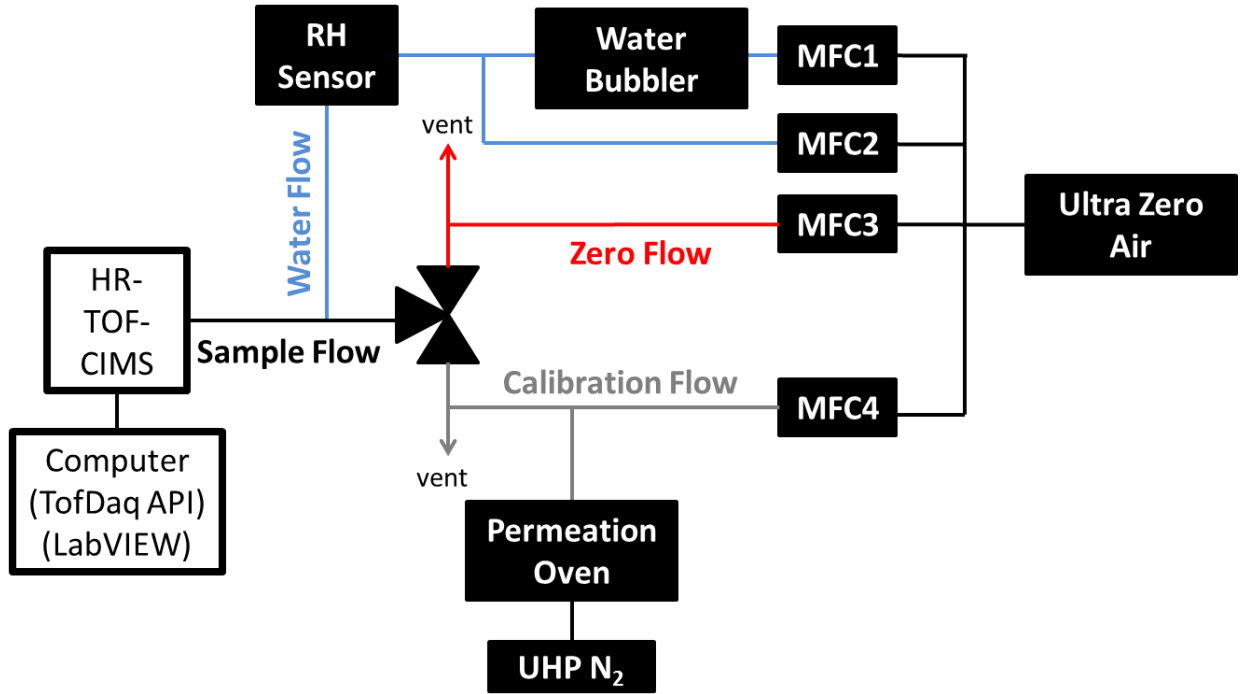


1 **SI 1: Experimental Setup**

2



3

4

5

6 Figure SI1: Schematic diagram of the automated experimental setup for used calibrating the HR-TOF-CIMS under
7 different voltage and humidity conditions.

8

9

10

11

12

13

14

15

16

17

18

19

20

21

22

23

24

25

26

27

28

29 **SI 2: Thuner determined voltage configuration starting point**

30

Table SII	
Initial Voltage Configuration (Thuner Derived)	
Component	Voltage
IMR Vacuum Region (100 mbar) SH-112 Agilent Single Scroll Pump	
IMR	-22
Short Segmented Quadrupole Region (2 mbar) Agilent TriScroll 600	
Nozzle	1.768
SSQ Entrance Plate	-2.766
SSQ Front	6.492
SSQ Back	4.196
Lens Skimmer	5.303
Skimmer	12
Big Segmented Quadrupole Region (1.3×10^{-3} mbar) Split Flow Pfeiffer Turbo Pump Stage 1	
BSQ Front	13
BSQ Back	13
Skimmer	20.194
Primary Beam Region (1.12×10^{-4}) Split Flow Pfeiffer Turbo Pump Stage 2	
Ref. (Bias)	56.617
Ion Lens	91.604
Deflector Flange	91.35
Deflector	95.25
Time-of-Flight Region (7.5×10^{-7} mbar) Split Flow Pfeiffer Turbo Pump Stage 3	
TOF Pulse	700
TOF Reference	43.895
TOF Extraction 1	30
TOF Extraction 2	700
TOF Lens	0
Drift	3000
Reflectron Grid	645.247
Reflectron Back	700
Post Acceleration	2800

31

32

33

34

35

36

37

38

39

40

41

42 **SI 2.1: Thuner Method General Setup**

43

44

45

46

47

48

49

50

51

52

53

54

55

56

57

58

59

60

61

62

63

64

65

66

67

68

69

70

71

72

73

74

75

76

77

78

79

The HR-TOF-CIMS continuously samples Ultra Zero Grade Air (Airgas, Inc.) to maintain stable signal across the mass range used for the Thuner experiments. Two zero air systems were also investigated (EnviroNics, Inc. and Aadco Instruments, Inc.), but these systems cause instabilities and are not suitable for long Thuner experiments (or most CIMS work in general). The set of voltages chosen to create all subsequent voltage configurations are shown in Table SI1.

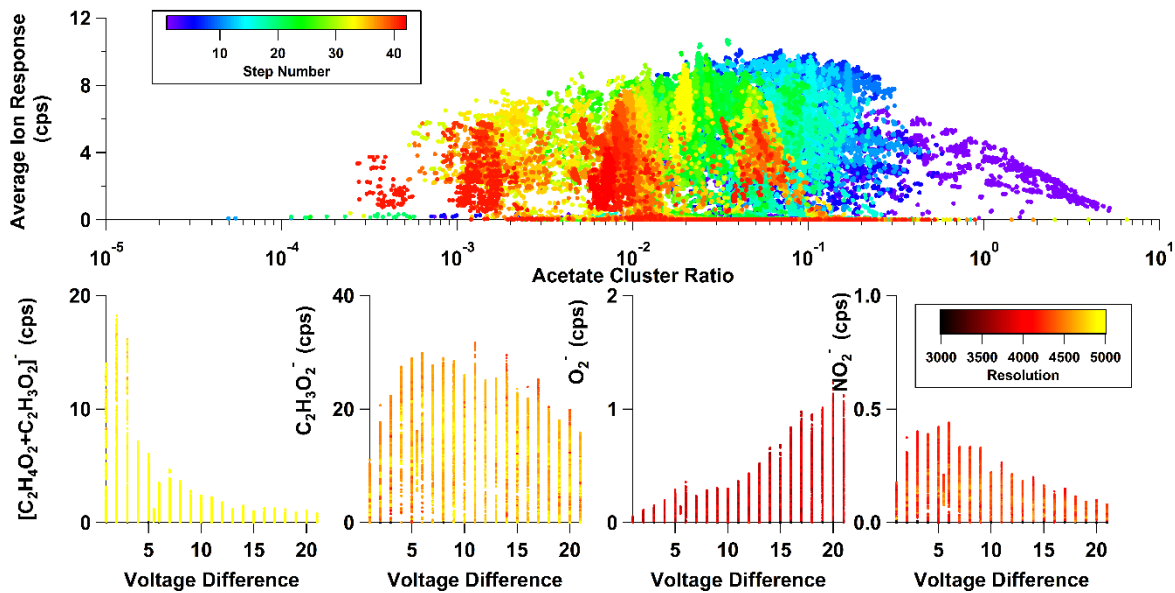
The approach to these Thuner experiments is to control clustering while optimizing the voltage configurations to maximize ion transmission efficiency. All of the controlling factors are summarized in Table SI2. All of the ions used for responses are summarized in Table SI3. The summary of results is presented in Figure SI1. Cluster control is primarily accomplished by controlling the voltage difference between the BSQ front and last skimmer in the SSQ (component relation 5) because this set of components is most sensitive towards controlling cluster transmission. The ions used to track sensitivity are all deprotonated-declustered ions. The idea is that cluster transmission is essentially held constant at each tuning step by constraining the system at component relation 5. Then the absolute ion transmission efficiency can be improved by monitoring the chosen ions. This is not exactly correct because other components can float to high or low voltage differences leading to more or less declustered operation; this can be overcome by more constrained control over the various API component relations. This effect is practically dealt with by simply post-processing the Thuner results and using the ratio between the signal of the [acetate + acetic acid] cluster and the acetate ion as the filtering criteria for choosing the voltage files.

Figure S1 (top) shows all the voltage experiments for the complete Thuner experiment. Each step is repeated 10 times with small allowable voltage ranges applied to each component. This allows Thuner to test voltage sets within a fairly small voltage space where optimizations are better constrained. The skimmer to BSQ voltage difference is changed after tuning the SSQ, BSQ, and TOF voltages using a single voltage range. Seven voltage ranges are used (0-3 V, 4-6 V, 7-9 V, 10-12 V, 13-15 V, 16-18 V, and 19-21 V).

The observed decrease in average ion signal at high clustering ratios arises from the choice of response ions being deprotonated-declustered ions. Much less acetate makes it through the API because a large fraction of the acetate ion is bound up in clustering reactions. This can be seen in the Figure SI1 (bottom panel) specifically examining the [acetate + acetic acid] cluster and acetate. At low voltage differences (high acetate cluster ratio) there is a huge signal from [acetate + acetic acid] cluster which rapidly decreases as a function of voltage difference. The opposite trend is true for acetate.

These considerations highlight the difficulty of tuning the API with Thuner. Two possible approaches exist for future investigations: highly constrained tuning and highly targeted tuning. This manuscript (main paper) shows that the various components in the API have knowable relationships, and their effects are only observed under certain voltage differences. Thus, it seems possible to tune while keeping all these voltage differences within certain ranges that will not significantly contribute to either relative ion transmission effects (e.g. voltage differences across the quadrupoles) or declustering effects. Then a single component relationship (skimmer to BSQ front) may be used to control clustering. The other, and probably simpler option, is to let Thuner to the work by targeting certain performance criteria. Acetate, formate, and chloride are used as response variables in the work discussed here.

80 Alternatively, one could define the acetate cluster ratio and use this number as a specific target. Key components can
81 still be constrained using this targeted mode of tuning.
82



83
84 Figure SI2: Thuner results of various ions and average response. Each point is one voltage configuration. Top: the
85 average ion response is colored by the Thuner step number and plotted as a function of the acetate cluster ratio.
86 Bottom: The average ion response of individual species is plotted as a function of applied voltage difference
87 between the last skimmer of the SSQ vacuum region and the BSQ entrance. These data are colored by the resolution
88 of the detected peak.

89
90
91
92
93
94
95
96

**Table S12
Thuner API Voltage Relations**

Step 1: SSQ Tuning Step			
Relationship Name	Components	Vacuum Region	Comments
IMR	IMR	IMR	
Nozzle	Nozzle	IMR to SSQ	
SSQ Entrance Plate	SSQ Entrance Plate	SSQ	
SSQ Average	(SSQ front + SSQ Back)/2	SSQ	Average voltage of SSQ
SSQ Difference	SSQ Back – SSQ Front	SSQ	Voltage drop across SSQ
Lens Skimmer	Lens Skimmer	SSQ	
SSQ-BSQ Transition	BSQ Front – Skimmer	SSQ to BSQ	Voltage drop from last SSQ region skimmer to BSQ front
BSQ Average	(BSQ front + BSQ Back)/2	BSQ	Average voltage of BSQ
BSQ Difference	BSQ Back – BSQ Front	BSQ	Voltage drop across BSQ
Step 2: BSQ/PB Tuning Step			
Lens Skimmer	Lens Skimmer	SSQ	
SSQ-BSQ Transition	BSQ Front – Skimmer	SSQ-BSQ	Voltage drop from last SSQ region skimmer to BSQ front
BSQ Average	(BSQ front + BSQ Back)/2	BSQ	Average voltage of BSQ
BSQ Difference	BSQ Back – BSQ Front	BSQ	Voltage drop across BSQ
Skimmer 2	Skimmer 2	BSQ	
Reference	Reference	PB	
Deflector Average	(deflector + deflector flange)/2	PB	Average voltage of lens stack
Deflector Difference	deflector flange – deflector	PB	Difference of lens stack
Lens	Lens	TOF	
Step 3: PB/TOF Tuning			
Reference	Reference	PB	
Deflector Average	(deflector + deflector flange)/2	PB	Average voltage of lens stack
Deflector Difference	deflector flange – deflector	PB	Difference of lens stack
Lens	Lens	TOF	
TOF Extraction Pulse 1	TOF Extraction Pulse 1	TOF	
TOF Extraction Reference	TOF Extraction Reference	TOF	
Reflectron Grid	Reflectron Grid	TOF	

97

98

99

100

Table SI3 Thuner Ions		
All Tuning Steps		
Ion	Used for m/z calibration	Used for sensitivity response
O ₂ ⁻	Yes	No
Cl ⁻	Yes	Yes
CHO ₂ ⁻	Yes	Yes
NO ₂ ⁻	Yes	No
CH ₃ CO ₂ ⁻ (Acetate Reagent Ion)	Yes	Yes
NO ₃ ⁻	Yes	No
C ₄ H ₇ O ₄ ⁻ (Acetate Reagent Cluster)	Yes	No

101

102

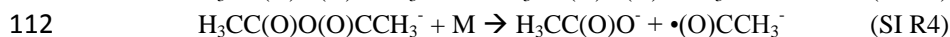
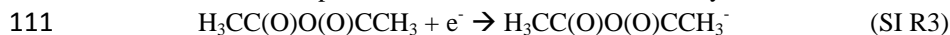
103

104 **SI 3: Proposed mechanism for observed [**•C₂H₃O₅** + Acetate]⁻ cluster**

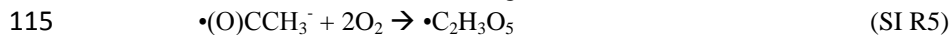
105

106 Alpha-particle emission from ²¹⁰Po

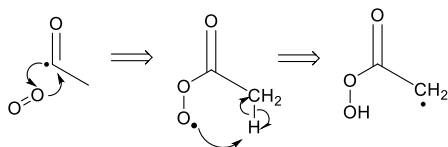
109

110 Electron capture and dissociation of Acetic Anhydride

113

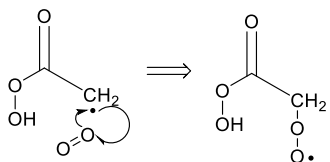
114 Auto-oxidation of radical fragment

116

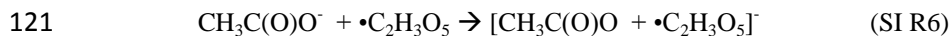


117

118



119

120 Cluster Formation of Radical

122

123

124

125

126

127

128

129

130

131

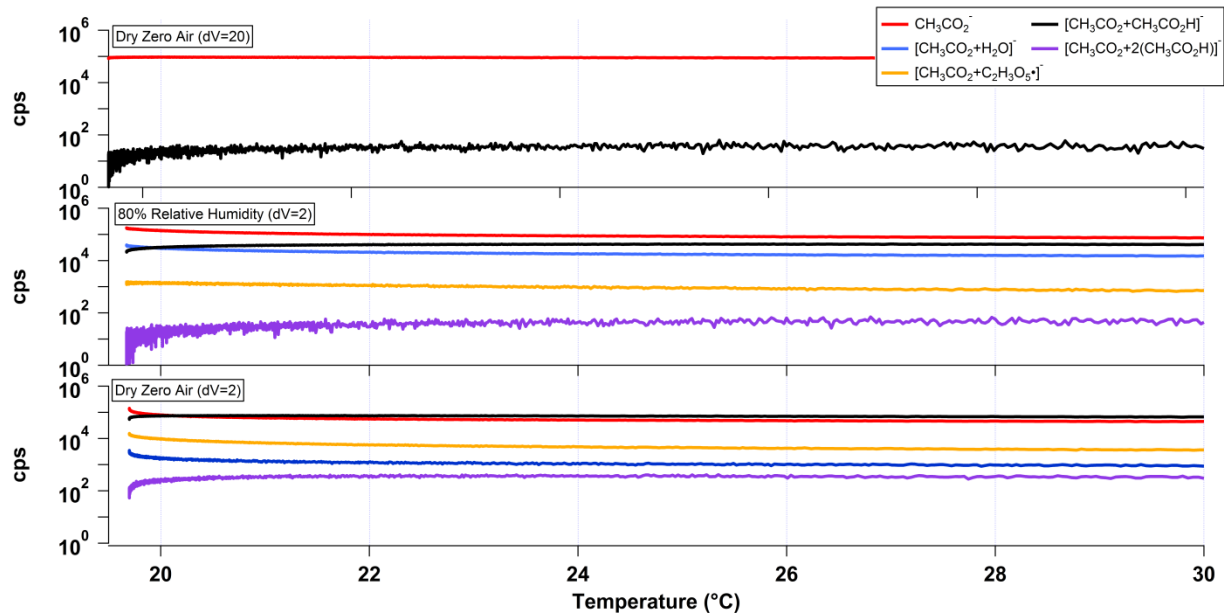
132 **SI 4: Effect of [acetic anhydride] on observed background spectra and reagent ions**

133 Bertram *et al.* (2011) show a mass spectrum with an [acetate + acetic acid]/acetate ratio of 5.54 and an
134 [acetate + 2(acetic acid)]/acetate ratio of 0.83. Both of these clusters are in much higher abundance in that study than
135 has ever been observed on our instrument. Additionally, the peak at m/z 166 corresponds to $[\text{CH}_3\text{C}(\text{O})\text{O} +$
136 $\bullet\text{C}_2\text{H}_3\text{O}_5]$ in our system. This peak is observed by Bertram *et al.* (2011), but is very small compared to the [acetate +
137 2(acetic acid)] cluster. Thus, API tuning alone probably does not explain the differences observed between our
138 instruments because one would assume that the $[\text{CH}_3\text{C}(\text{O})\text{O} + \bullet\text{C}_2\text{H}_3\text{O}_5]$ cluster would be transmitted easily given
139 the abundance of the higher order cluster.

140 The amount of acetic anhydride added to these systems remains a difficult number to constrain because
141 liquid filled reservoirs are routinely used to generate acetate reagent ions. We attempted heating and cooling
142 experiments that show subtle changes in the abundance and ratio of the dominate species produced from acetate
143 CIMS. Figure SI3 shows the experimental results. Briefly, the acetic anhydride glass reservoir, stainless steel
144 transfer lines, and Po-210 ionizer are constantly heated using heating rope and a PID temperature controller during
145 normal operation. This entire heating system is turned off during this experiment and allowed to cool while the HR-
146 TOF-CIMS continues acquiring mass spectra. This experiment is conducted under two voltage configurations (high
147 declustering mode $dV=20$ and cluster mode $dV=2$) and two relative humidity settings (0% and 80% RH).

148 No change is observed under declustered settings further highlighting the importance of running this
149 instrument in cluster mode to understand the underlying ion-neutral chemistry occurring in the IMR. Operation
150 under cluster mode shows significant changes. Under dry conditions, the [acetate + 2(acetic acid)] cluster and the
151 [acetate + water] cluster are observable but very small. Increasing the temperature (more acetic anhydride) leads to
152 an increase in both the [acetate + acetic acid] and [acetate + 2(acetic acid)] clusters while slightly decreasing the
153 $[\text{CH}_3\text{C}(\text{O})\text{O} + \bullet\text{C}_2\text{H}_3\text{O}_5]$ cluster. Under high relative humidity conditions, the [acetate + 2(acetic acid)] is very small
154 and barely detectable. The [acetate + water] and $[\text{CH}_3\text{C}(\text{O})\text{O} + \bullet\text{C}_2\text{H}_3\text{O}_5]$ clusters decreases as more acetic
155 anhydride is added to the Po-210 ionizer. It is not expected that adding huge amounts of acetic anhydride will ever
156 be sufficient to titrate out the [acetate+water] cluster because it makes up a very large fraction of the total signal.

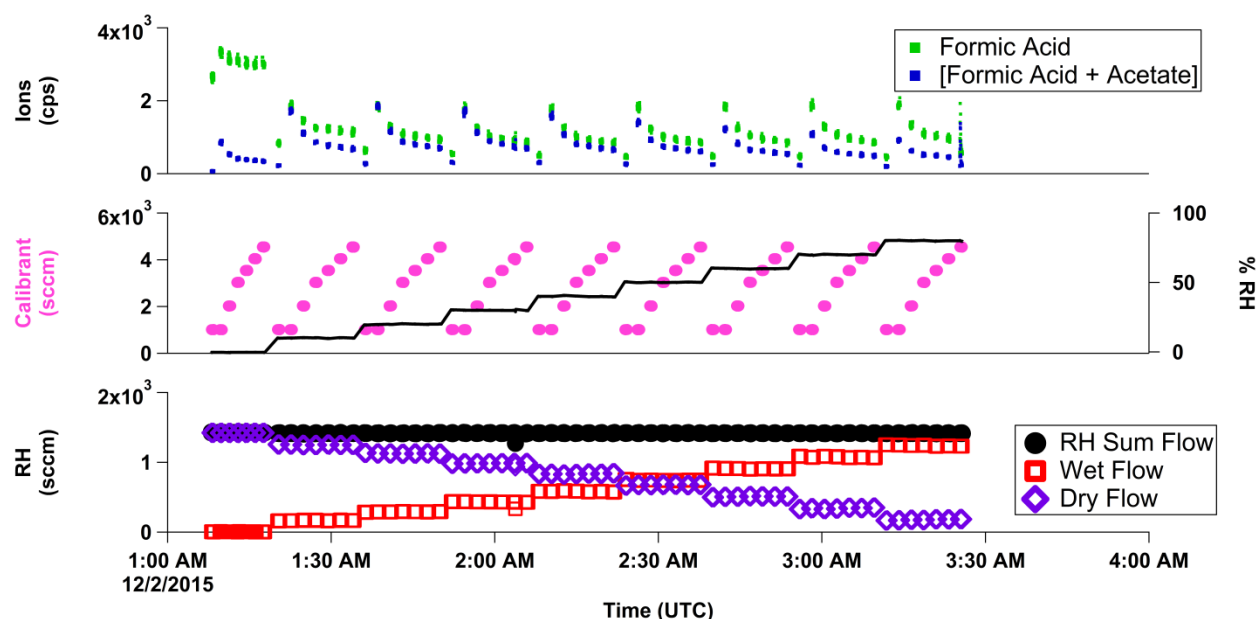
157



158
 159 Figure SI3: The effect of heating and cooling the acetic anhydride reservoir and transfer lines on the observed
 160 reagent ion signals. The heating/cooling cycle is conducted under declustered settings (top) and clustered settings
 161 (middle and bottom). Relative humidity is set to 80% under cluster mode (middle) for comparison to dry
 162 experiments under cluster mode (bottom).

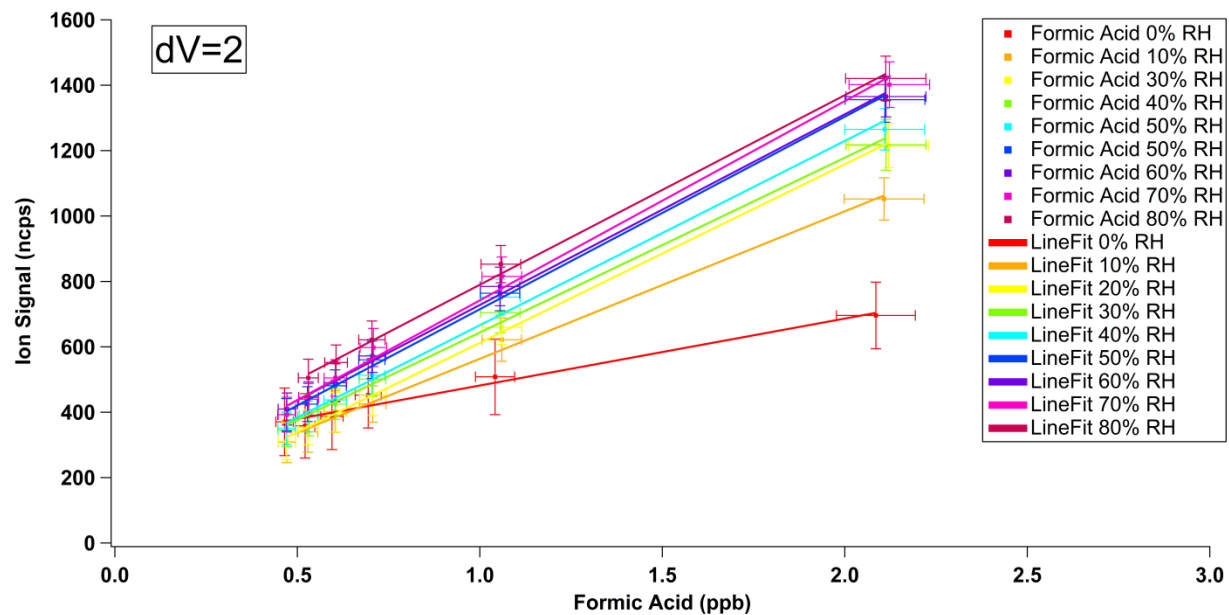
163
 164
 165
 166
 167
 168
 169
 170
 171
 172
 173
 174
 175
 176
 177
 178
 179
 180
 181
 182
 183
 184
 185
 186
 187
 188

189 **SI 5: Other calibrations and additional data**



190
 191 Figure SI4: Detailed summary of experimental calibration procedure for voltage and relative humidity dependent
 192 calibrations. (Bottom) Relative humidity control system: the flow from the MFC pushing ultra zero air through a
 193 series of water filled glass bubblers and the flow from the MFC controlling the dry air flow. The sum of these two
 194 controllers is held constant. (Middle) The resulting relative humidity generated from the relative humidity control
 195 system measured from the inline relative humidity sensor is plotted on the right axis. The MFC controlling the
 196 dilution flow of the calibration source is plotted on the left axis. (Top) The ion signal is shown for formic acid and
 197 the [acetate + formic acid] cluster during the calibration experiment.

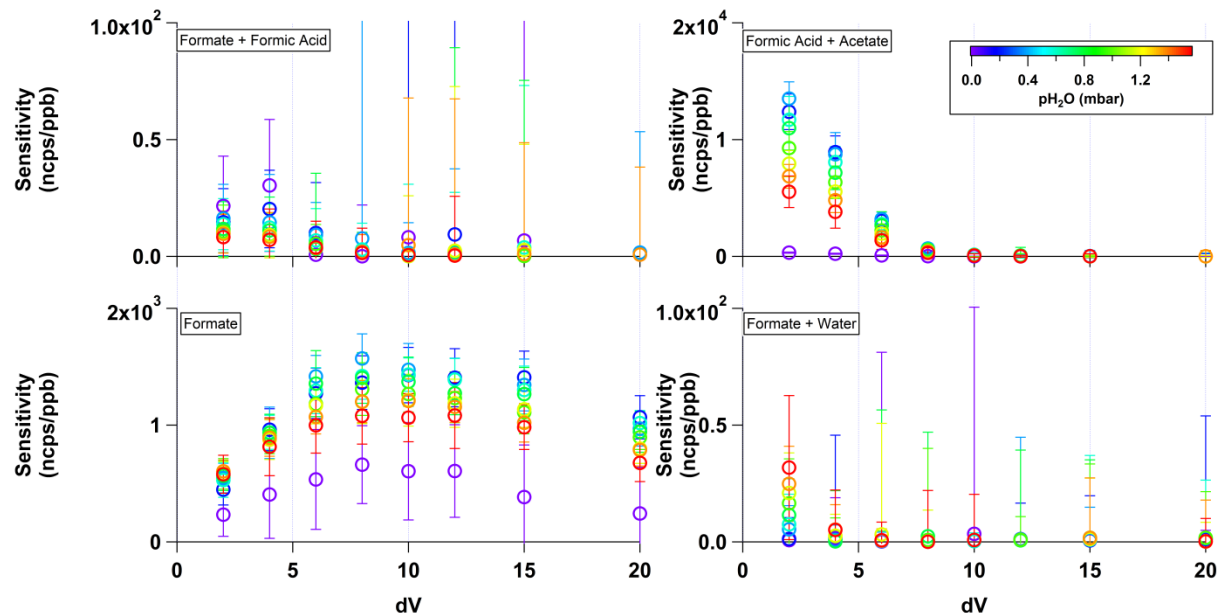
198
 199
 200
 201
 202



203
 204 Figure SI5: Normalized and background subtracted calibration curves colored by relative humidity and collected
 205 under a single voltage configuration using the experimental setup graphically described in Figure SI3. These data are
 206 automatically generated for all species investigated. Deprotonated-declustered formic acid is shown here.

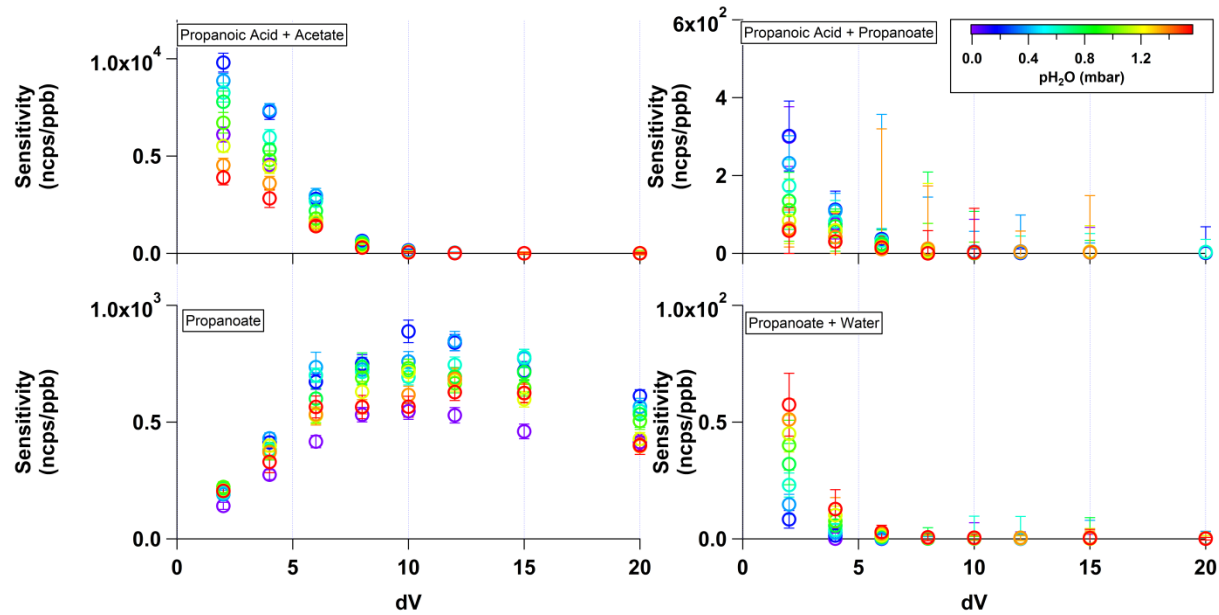
207
 208
 209
 210
 211
 212
 213
 214
 215
 216
 217
 218
 219
 220
 221
 222
 223
 224
 225
 226
 227
 228
 229
 230
 231
 232
 233

234 SI 5.1 Sensitivity
235



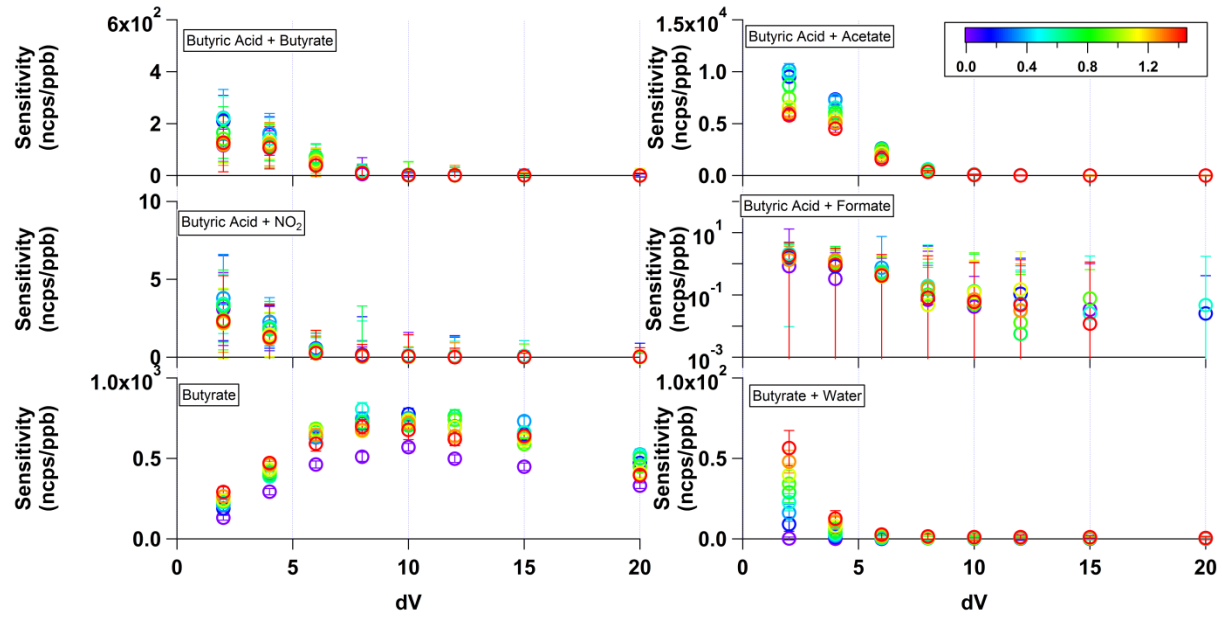
236
237 Figure SI6: The sensitivity to formic acid and related clusters is plotted against the voltage difference applied
238 between the skimmer and BSQ front (component relation 5). The points are colored by the calculated partial
239 pressure of water in the IMR corresponding to changing the relative humidity from 0% to 80% under laboratory
240 conditions. Sensitivity drops off at higher dV values for clustered species but is maintained for declustered-
241 deprotonated ions.

242
243
244



245
 246 Figure SI7: The sensitivity to propanoic acid and related clusters is plotted against the voltage difference applied
 247 between the skimmer and BSQ front (component relation 5). The points are colored by the calculated partial
 248 pressure of water in the IMR corresponding to changing the relative humidity from 0% to 80% under laboratory
 249 conditions. Sensitivity drops off at higher dV values for clustered species but is maintained for declustered-
 250 deprotonated ions.

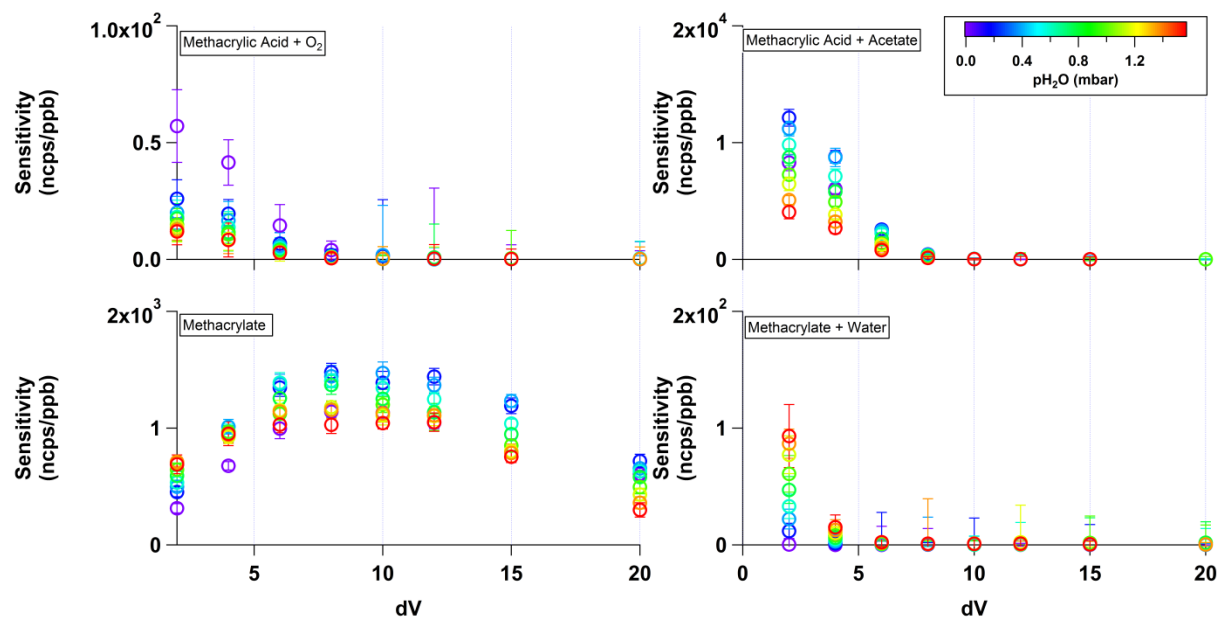
251
 252
 253
 254
 255
 256
 257



258

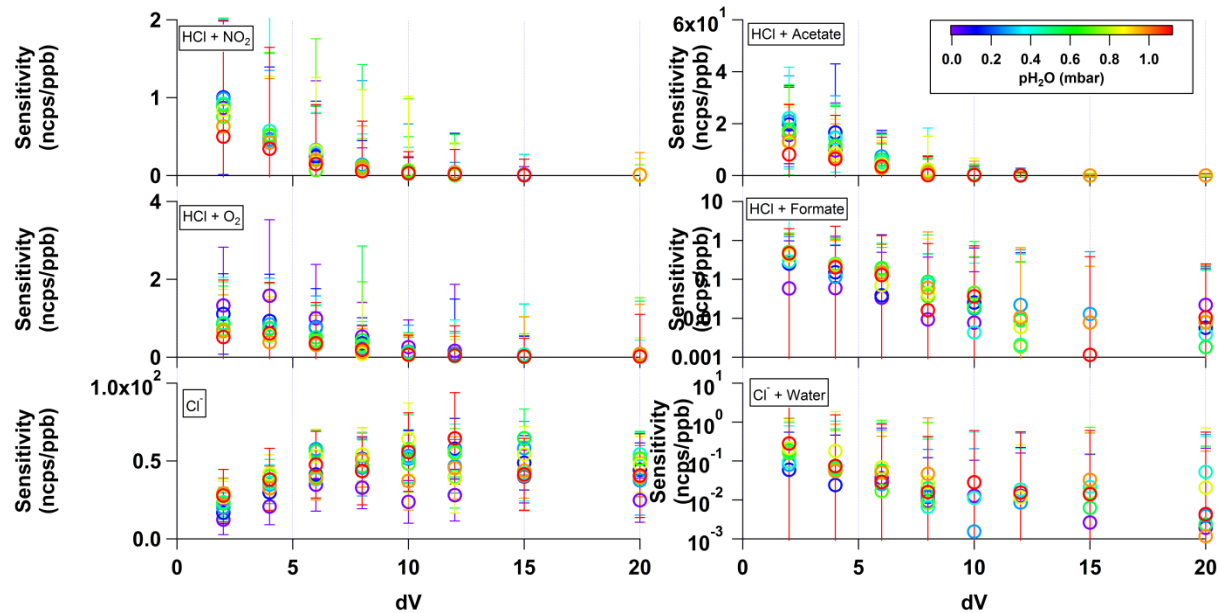
259 Figure SI8: The sensitivity to butyric acid and related clusters is plotted against the voltage difference applied
 260 between the skimmer and BSQ front (component relation 5). The points are colored by the calculated partial
 261 pressure of water in the IMR corresponding to changing the relative humidity from 0% to 80% under laboratory
 262 conditions. Sensitivity drops off at higher dV values for clustered species but is maintained for declustered-
 263 deprotonated ions.

264
 265
 266
 267
 268
 269



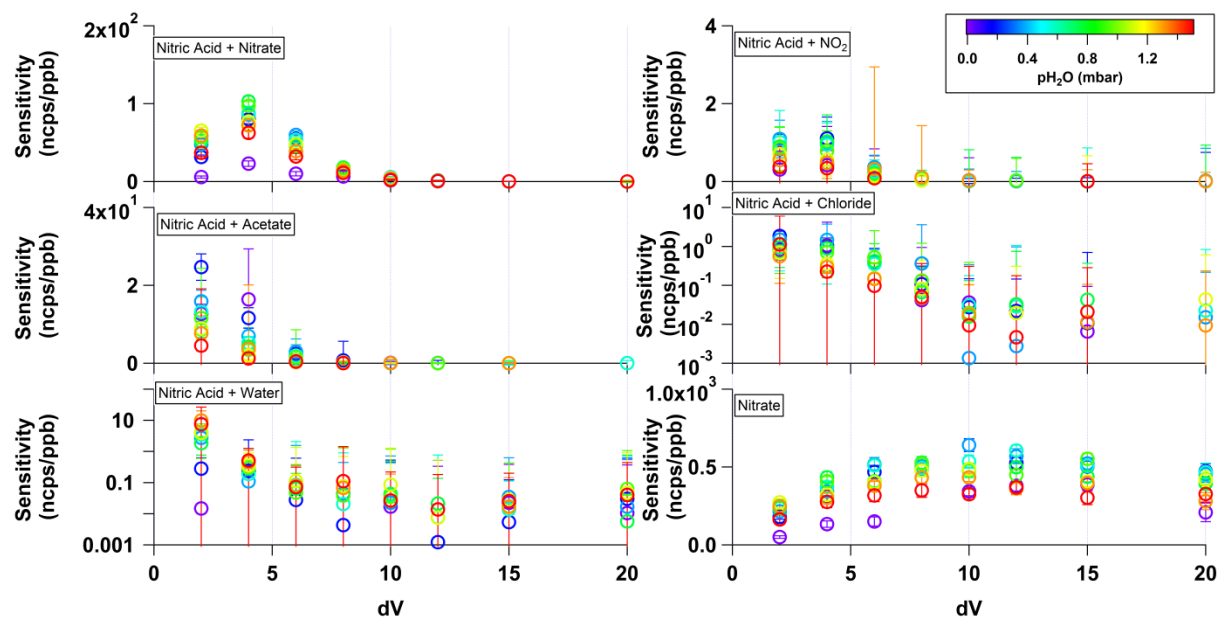
270
 271 Figure SI9: The sensitivity to methacrylic acid and related clusters is plotted against the voltage difference applied
 272 between the skimmer and BSQ front (component relation 5). The points are colored by the calculated partial
 273 pressure of water in the IMR corresponding to changing the relative humidity from 0% to 80% under laboratory
 274 conditions. Sensitivity drops off at higher dV values for clustered species but is maintained for declustered-
 275 deprotonated ions.

276
 277
 278
 279
 280
 281
 282



283
 284 Figure SI10: The sensitivity to hydrochloric acid and related clusters is plotted against the voltage difference applied
 285 between the skimmer and BSQ front (component relation 5). The points are colored by the calculated partial
 286 pressure of water in the IMR corresponding to changing the relative humidity from 0% to 80% under laboratory
 287 conditions. Sensitivity drops off at higher dV values for clustered species but is maintained for declustered-
 288 deprotonated ions.

289
 290
 291
 292
 293
 294



295

296 Figure S11: The sensitivity to nitric acid and related clusters is plotted against the voltage difference applied
 297 between the skimmer and BSQ front (component relation 5). The points are colored by the calculated partial
 298 pressure of water in the IMR corresponding to changing the relative humidity from 0% to 80% under laboratory
 299 conditions. Sensitivity drops off at higher dV values for clustered species but is maintained for declustered-
 300 deprotonated ions.

301
 302
 303
 304
 305
 306
 307
 308
 309
 310
 311
 312
 313
 314
 315
 316
 317
 318
 319
 320
 321
 322
 323

324 **SI 5.2 Sensitivity Ratios**

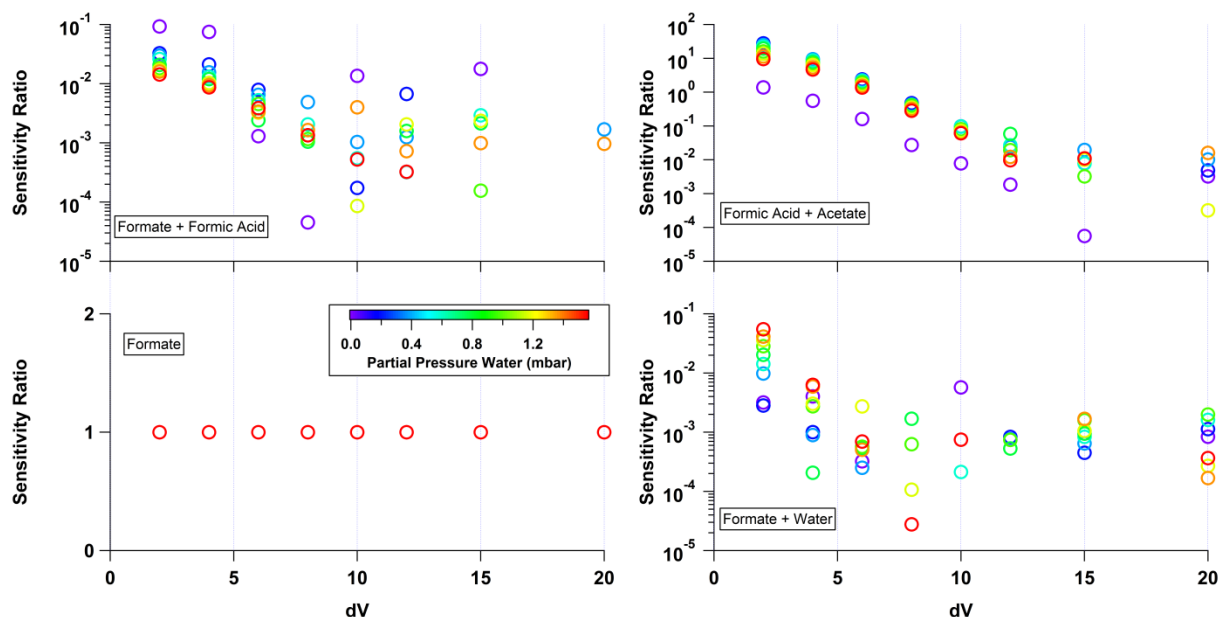
325

326 Sensitivity Ratio = $\frac{S_{RH,dV}[RC(O)OH+X]}{S_{RH,dV}(RC(O)O^-)}$ (SI Eqn. 1)

327

328 The sensitivity ratio is defined as the sensitivity at some relative humidity and voltage configuration ($S_{RH,dV}$) of
 329 some cluster $[RC(O)OH+X]$ divided by the sensitivity at the same relative humidity and voltage configuration
 330 ($S_{RH,dV}$) of the deprotonated-declustered ion during the calibration $[RC(O)O^-]$. These plots (along with the LOD
 331 plots SI 4.3) show another way of examining how much a cluster can contribute to an observed signal relative to the
 332 signal of the identified deprotonated-declustered ion. It should be noted that if linear regression converges in the
 333 automated calibration curve processing script, it is included in this plot to provide an estimate of a calibration factor.
 334 At high dV values, many of the cluster calibration curves show poor r^2 values and the trend of decreasing sensitivity
 335 ratio as a function of dV will weaken.

336



337

338 Figure SI12: Sensitivity ratios of various formic acid clusters relative to the sensitivity of formic acid under a variety
 339 of relative humidity conditions and voltage configurations. The contribution of the formic acid clusters to the
 340 observed mass spectrum decreases relative to the contribution at the deprotonated-declustered mass as dV increases.

341

342

343

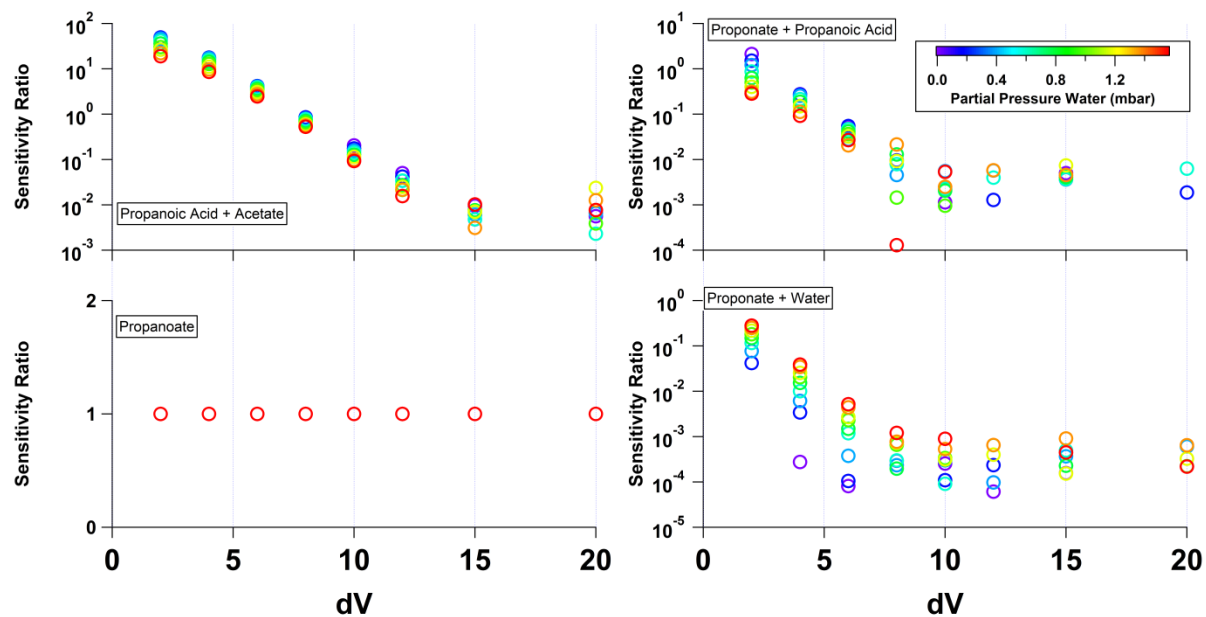
344

345

346

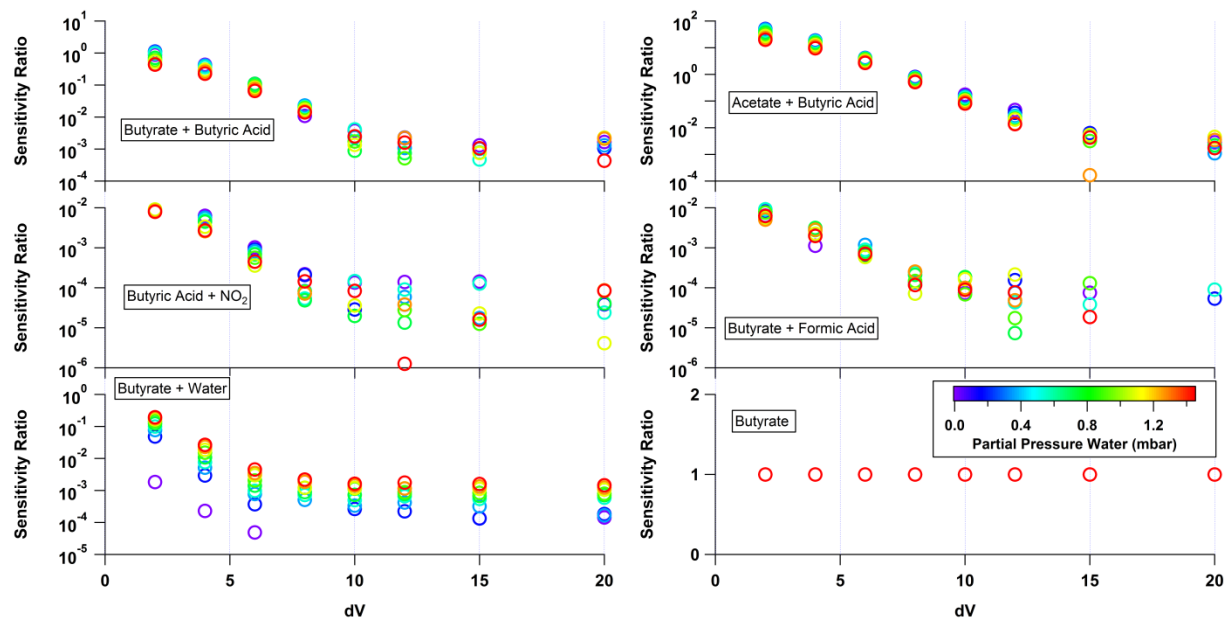
347

348



349
 350 Figure SI13: Sensitivity ratios of various propanoic acid clusters relative to the sensitivity of propanoic acid under a
 351 variety of relative humidity conditions and voltage configurations. The contribution of the propanoic acid clusters to
 352 the observed mass spectrum decreases relative to the contribution at the deprotonated-declustered mass as dV
 353 increases.

354
 355
 356
 357
 358
 359
 360
 361
 362
 363



364

365 Figure SI14: Sensitivity ratios of various butyric acid clusters relative to the sensitivity of butyric acid under a
 366 variety of relative humidity conditions and voltage configurations. The contribution of the butyric acid clusters to
 367 the observed mass spectrum decreases relative to the contribution at the deprotonated-declustered mass as dV
 368 increases.

369

370

371

372

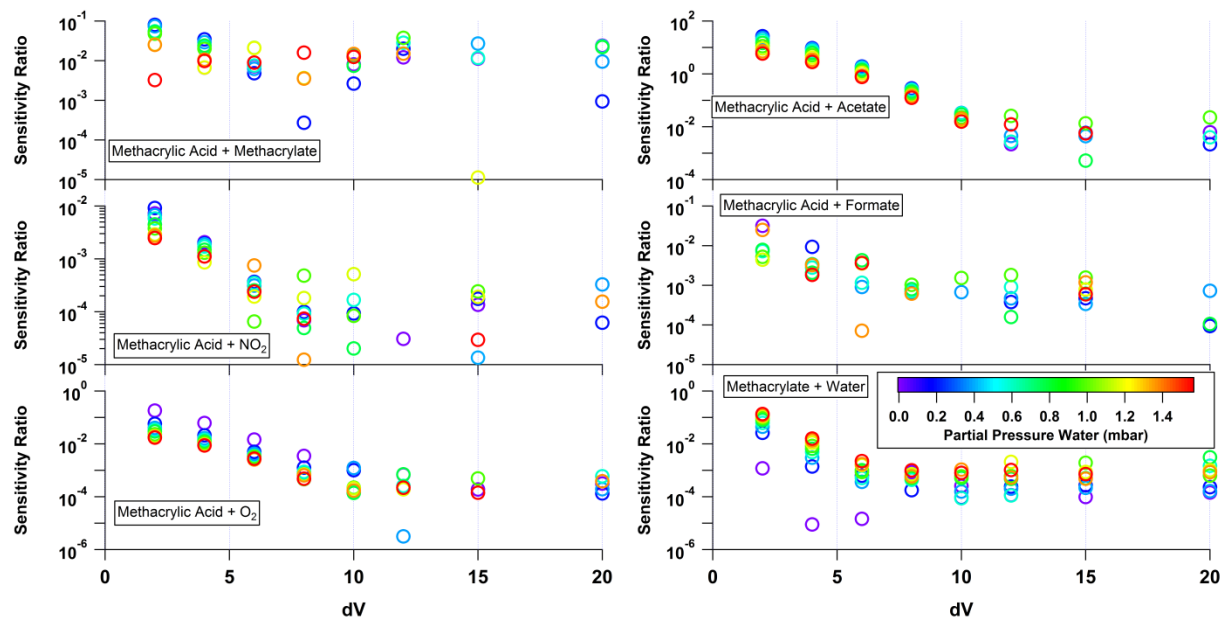
373

374

375

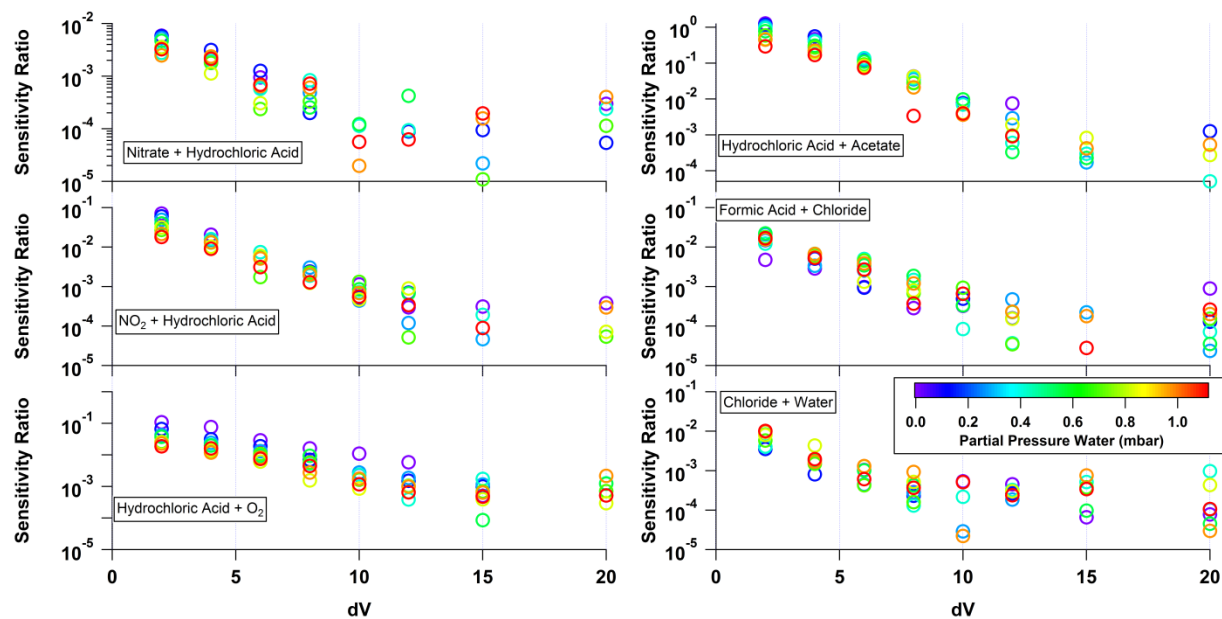
376

377



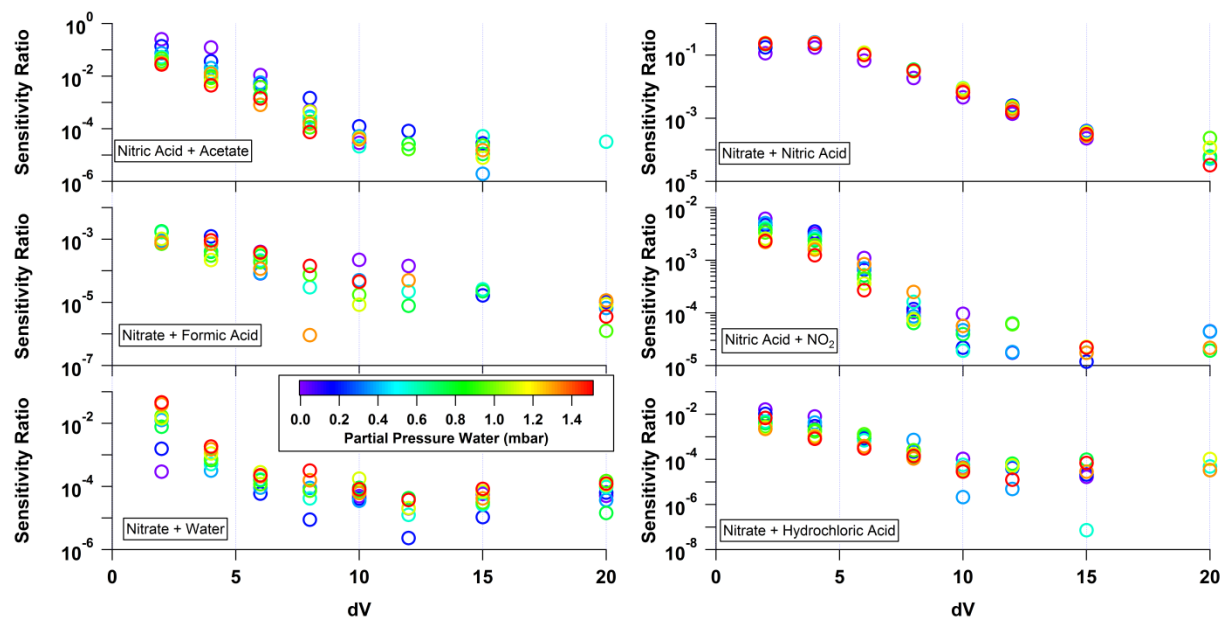
378
 379 Figure SI15: Sensitivity ratios of various methacrylic acid clusters relative to the sensitivity of methacrylic acid
 380 under a variety of relative humidity conditions and voltage configurations. The contribution of the methacrylic acid
 381 clusters to the observed mass spectrum decreases relative to the contribution at the deprotonated-declustered mass as
 382 dV increases. Here, the deprotonated-declustered methacrylate ion is removed (it always equals 1), and the
 383 methacrylic acid self-cluster is included.

384
 385
 386
 387
 388
 389



390
 391 Figure SI16: Sensitivity ratios of various hydrochloric acid clusters relative to the sensitivity of hydrochloric acid
 392 under a variety of relative humidity conditions and voltage configurations. The contribution of the hydrochloric acid
 393 clusters to the observed mass spectrum decreases relative to the contribution at the deprotonated-declustered mass as
 394 dV increases. Here, the deprotonated-declustered chloride ion is removed (it always equals 1), and the
 395 [nitrate+hydrochloric acid] cluster is included.

396
 397
 398
 399
 400
 401



402
 403 Figure SII7: Sensitivity ratios of various nitric acid clusters relative to the sensitivity of nitric acid under a variety of
 404 relative humidity conditions and voltage configurations. The contribution of the nitric acid clusters to the observed
 405 mass spectrum decreases relative to the contribution at the deprotonated-declustered mass as dV increases. Here, the
 406 deprotonated-declustered nitrate ion is removed (it always equals 1), and the [nitrate+formic] acid self-cluster is
 407 included.

408
 409
 410
 411
 412
 413
 414
 415
 416
 417
 418
 419
 420
 421
 422
 423
 424
 425
 426
 427
 428
 429
 430

431 **SI 5.3 Limit of Detection**

432

433 LOD: $S/N=3$

434

435
$$\frac{S}{N} = \frac{C_f[x]t}{\sqrt{C_f[x]t+2Bt}} \quad (\text{SI Eqn. 2})$$

436

437 The limit of detection (LOD) is calculated via SI Eqn. 2 following the work of Bertram *et al.* (2011) and application

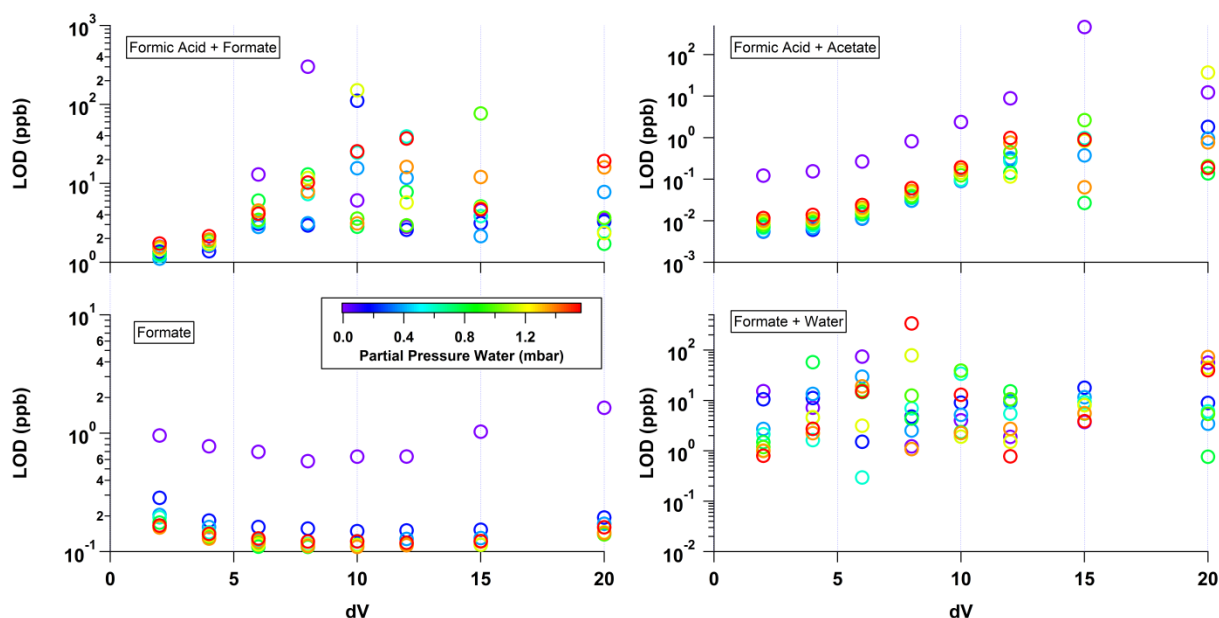
438 by Brophy and Farmer (2015). S/N is the signal-to-noise ratio, C_f is the calibration factor, $[x]$ is the mixing ratio, t is

439 the integration time, and B is the background count rate. This derivation assumes Poisson statistics. These plots

440 show at what concentration clustering is going to contribute to the observed mass spectrum with statistical

441 significance.

442



443

444 Figure SI18: The calculated 1 s ($S/N=3$) limit of detection of formic acid and related clusters is plotted against the

445 voltage difference applied between the skimmer and BSQ front (component relation 5). The points are colored by

446 the calculated partial pressure of water in the IMR corresponding to changing the relative humidity from 0% to 80%

447 under laboratory conditions. The limit of detection is observed to increase or become sporadic at higher dV values

448 for clusters while declustered-deprotonated species remain detectable at low concentrations.

449

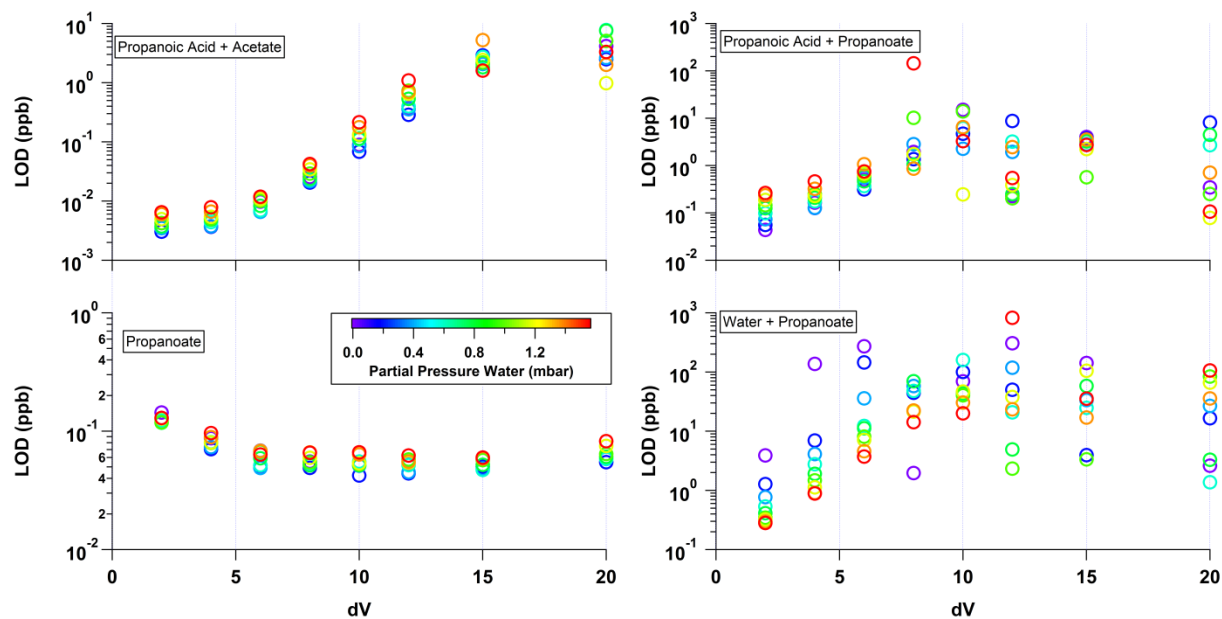
450

451

452

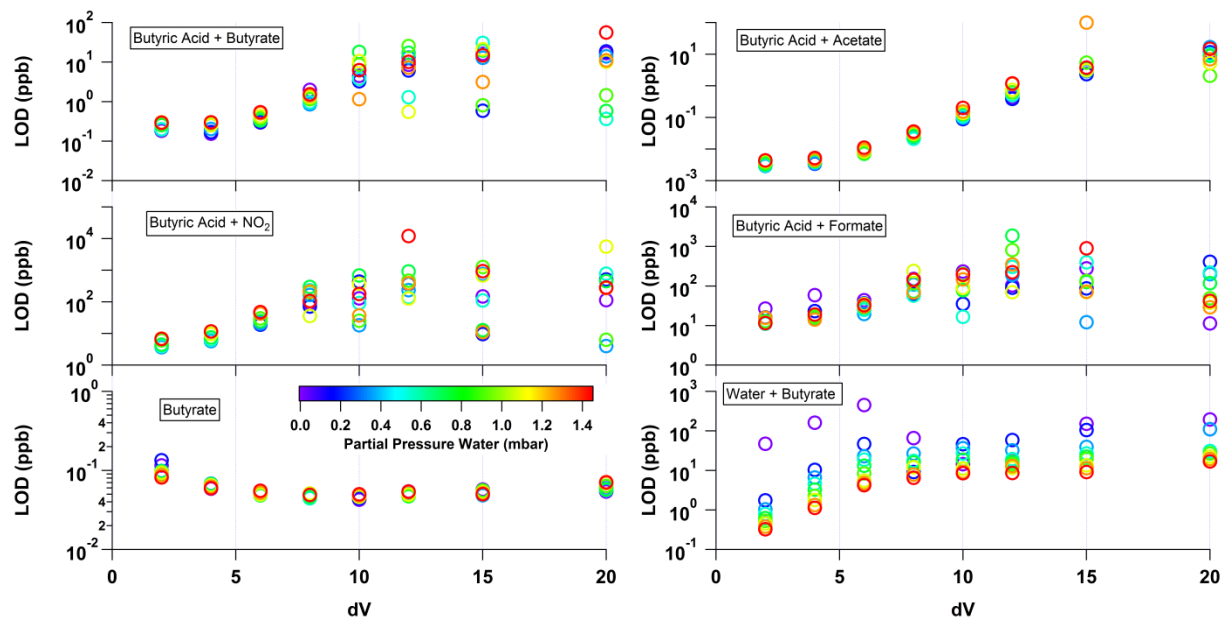
453

454



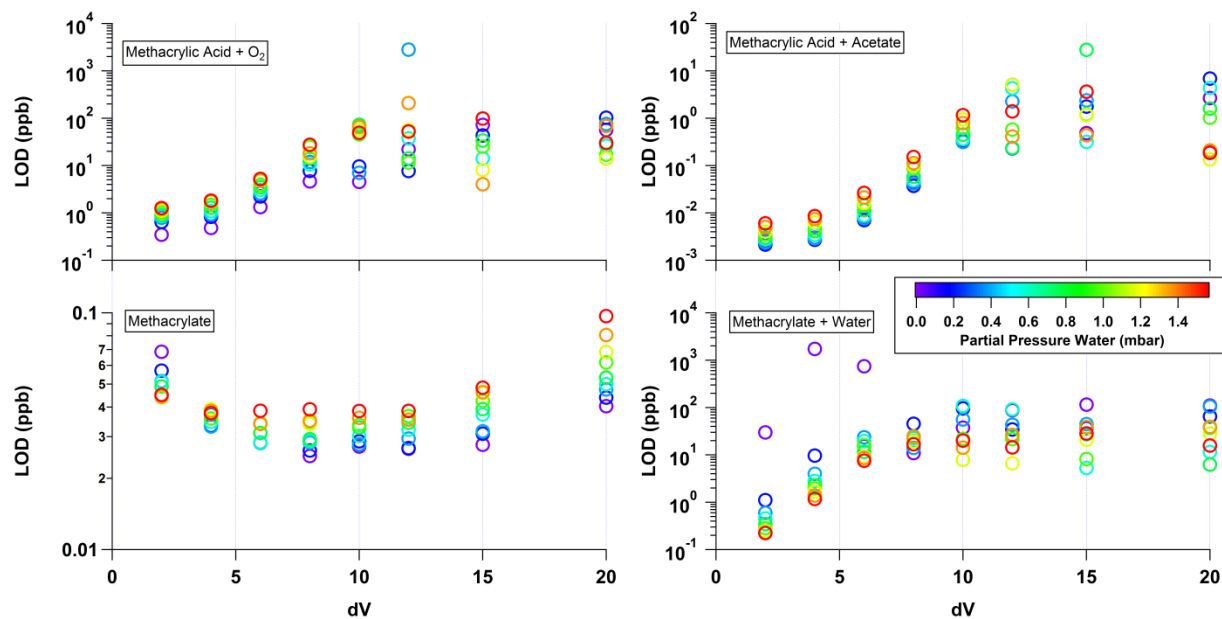
455
 456 Figure SI19: The calculated 1 s (S/N=3) limit of detection of propanoic acid and related clusters is plotted against
 457 the voltage difference applied between the skimmer and BSQ front (component relation 5). The points are colored
 458 by the calculated partial pressure of water in the IMR corresponding to changing the relative humidity from 0% to
 459 80% under laboratory conditions. The limit of detection is observed to increase or become sporadic at higher dV
 460 values for clusters while declustered-deprotonated species remain detectable at low concentrations.

461
 462
 463
 464
 465
 466
 467
 468
 469
 470
 471
 472
 473
 474



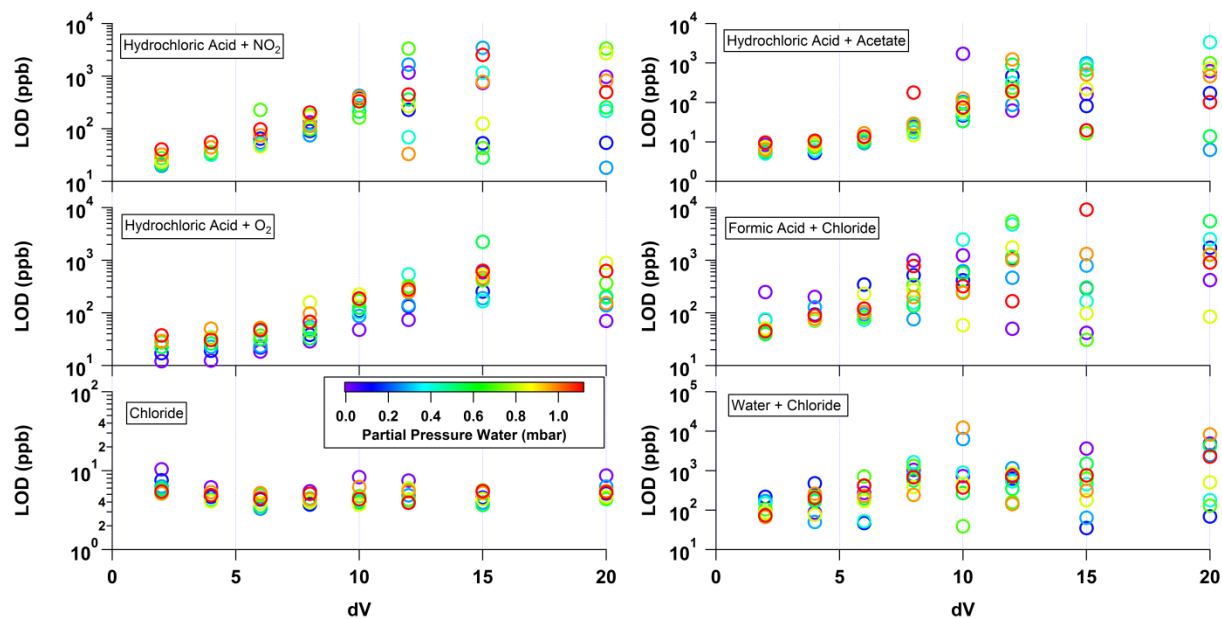
475
 476 Figure SI20: The calculated 1 s (S/N=3) limit of detection of butyric acid and related clusters is plotted against the
 477 voltage difference applied between the skimmer and BSQ front (component relation 5). The points are colored by
 478 the calculated partial pressure of water in the IMR corresponding to changing the relative humidity from 0% to 80%
 479 under laboratory conditions. The limit of detection is observed to increase or become sporadic at higher dV values
 480 for clusters while declustered-deprotonated species remain detectable at low concentrations.

481
 482
 483
 484
 485



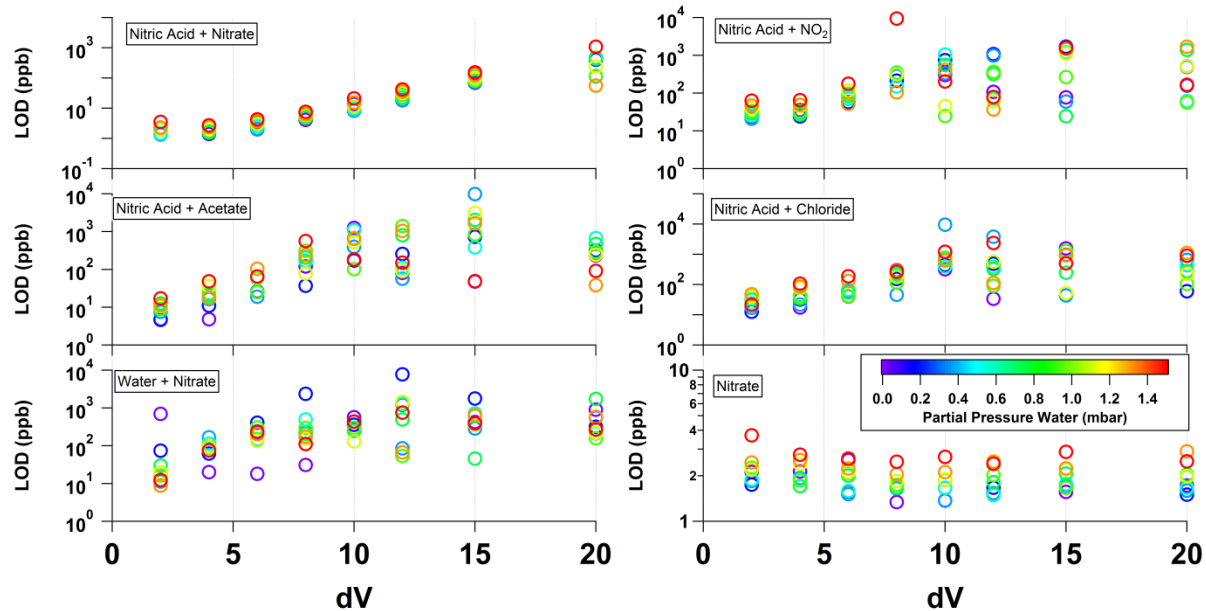
486
 487 Figure SI21: The calculated 1 s (S/N=3) limit of detection of methacrylic acid and related clusters is plotted against
 488 the voltage difference applied between the skimmer and BSQ front (component relation 5). The points are colored
 489 by the calculated partial pressure of water in the IMR corresponding to changing the relative humidity from 0% to
 490 80% under laboratory conditions. The limit of detection is observed to increase or become sporadic at higher dV
 491 values for clusters while declustered-deprotonated species remain detectable at low concentrations.

492
 493
 494
 495
 496



497
 498 Figure SI22: The calculated 1 s (S/N=3) limit of detection of hydrochloric acid and related clusters is plotted against
 499 the voltage difference applied between the skimmer and BSQ front (component relation 5). The points are colored
 500 by the calculated partial pressure of water in the IMR corresponding to changing the relative humidity from 0% to
 501 80% under laboratory conditions. The limit of detection is observed to increase or become sporadic at higher dV
 502 values for clusters while declustered-deprotonated species remain detectable at low concentrations.

503
 504
 505
 506
 507
 508
 509



510
 511 Figure SI23: The calculated 1 s (S/N=3) limit of detection of nitric acid and related clusters is plotted against the
 512 voltage difference applied between the skimmer and BSQ front (component relation 5). The points are colored by
 513 the calculated partial pressure of water in the IMR corresponding to changing the relative humidity from 0% to 80%
 514 under laboratory conditions. The limit of detection is observed to increase or become sporadic at higher dV values
 515 for clusters while declustered-deprotonated species remain detectable at low concentrations.

516
 517
 518
 519
 520
 521
 522
 523
 524
 525
 526
 527
 528
 529
 530
 531
 532
 533
 534
 535
 536
 537
 538
 539

540 **SI6: Evaluation of Chhabra Method for Dealing with Cluster Contributions**

541 Chhabra et al. (2015) formulate the expression that the clustered mass intensity ($I_{i+\text{acetate}}$) is equal to the sum of the
542 cluster (I_i) plus a non-clustered ion with the same exact mass (I_j). Thus:

543

544
$$I_{i+\text{acetate}} = I_i + I_j \quad (\text{SI Eqn. 3})$$

545

546 Next, the authors assume that the ratio between I_i and I_j is constant and no more than the acetate ratio of 0.2 in their
547 study. Either the $I_{i+\text{acetate}}$ to I_i ratio, or 0.2 is used (whichever value is smaller) to determine the contribution of the
548 clustered species to the mass $I_{i+\text{acetate}}$.

549

550
$$I_i \approx (I_{i+\text{acetate}}/I_i) \times I_j \quad \text{OR} \quad I_i \approx 0.2 \times I_j \quad (\text{SI Eqn. 4})$$

551

552 An acetate ratio of 0.2 in our system corresponds to operating component relation 5 at a dV of ~6 V (actual acetate
553 ratio of 0.16). Here, the relative contribution of propionic acid to the [propionic acid + acetate]⁻ cluster ranges
554 between 2.47 and 4.15 depending on the relative humidity. The relative contribution of formic acid to the [formic
555 acid + acetate]⁻ cluster ranges between 0.16 to 2.38. The relative contribution of butyric acid to the [butyric acid +
556 acetate]⁻ cluster ranges between 2.67 and 4.1. The relative contribution of methacrylic acid to the [methacrylic acid
557 + acetate]⁻ cluster ranges between 0.77 and 1.89. The self-cluster of propionic acid contributes only 0.054 and the
558 water-cluster contributes an order of magnitude less relative to the deprotonated-declustered sensitivity. This is a
559 consistent story for all the alkanolic acids evaluated. Nitric acid provides an interesting example. The [nitric acid +
560 acetate]⁻ cluster contributes between 0.011 and 0.008 relative to the nitrate signal while the nitric acid self-cluster
561 contributes between 0.12 and 0.06 relative to nitrate. This self-cluster is not addressed by these recommendations.

562